Title

Probing the Dynamics of Rydberg and Valence States of Molecular Nitrogen with Attosecond Transient Absorption Spectroscopy

Journal

The Journal of Physical Chemistry A, 120(19)

ISSN

1089-5639

Authors

Warrick, Erika R
Cao, Wei
Neumark, Daniel M
et al.

Publication Date

2016-05-19

DOI

10.1021/acs.jpca.5b11570

Peer reviewed

THE JOURNAL OF PHYSICAL CHEMISTRY A

Article

pubs.acs.org/JPCA

Probing the Dynamics of Rydberg and Valence States of Molecular Nitrogen with Attosecond Transient Absorption Spectroscopy

Erika R. Warrick,[†,‡] Wei Cao,[†] Daniel M. Neumark,[*,†,‡] and Stephen R. Leone[*,†,‡,§]

[†]Chemical Sciences Division, Lawrence Berkeley National Laboratory, Berkeley, California 94720, United States

[‡]Department of Chemistry, University of California, Berkeley, California 94720, United States

[§]Department of Physics, University of California, Berkeley, California 94720, United States

ABSTRACT: An attosecond pulse is used to create a wavepacket in molecular nitrogen composed of multiple bound and autoionizing electronic states of Rydberg and valence character between 12 and 16.7 eV. A time-delayed, few-femtosecond, near-infrared (NIR) laser pulse is used to couple individual states in the wavepacket to multiple neighboring states, resulting in time-dependent modification of the absorption spectrum and revealing both individual quantum beats of the wavepacket and the energy shifts of the excited states in the presence of the strong NIR field. The broad bandwidth of the attosecond pulse and high energy resolution of the extreme ultraviolet spectrometer allow the simultaneous observation of time-dependent dynamics for many individual vibrational levels in each electronic state. Quantum beating with periods from 1.3 to 12 fs and transient line shape changes are observed among vibrational levels of a progression of electronically autoionizing Rydberg states leading to the excited $A\ ^2\Pi_u\ N_2^+$ ion core. Vibrational levels in the valence $b\ ^1\Pi_u$ state exhibit 50 fs oscillation periods, revealing superpositions between individual vibrational levels within this state. Comparisons are made to previous studies of electronic wavepackets in atoms that highlight similarities to atomic behavior yet illustrate unique contributions of the diatomic molecular structure to the wavepacket, including the influence of different electronic potentials and vibrational-level-specific electronic dynamics.

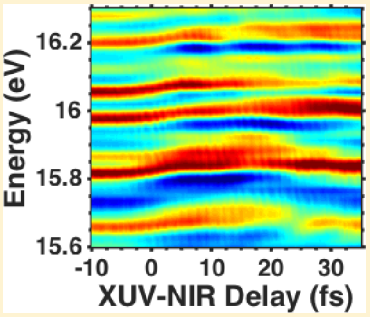

1. INTRODUCTION

Coherent superpositions, also known as wavepackets, of rotational, vibrational, or electronic states of an atomic or molecular system can be prepared and manipulated using laser pulses to produce selective dynamics. Intriguing examples include the control of products formed in a chemical reaction using multiple light pulses to create and probe a vibrational superposition[1,2] and the use of rotational wavepackets to create field free alignment of a target.[3] Because the creation and evolution of a wavepacket depends on the energy level spacing, historically these studies have been limited to the relatively narrow bandwidths of femtosecond or picosecond lasers. Wavepackets consisting of widely separated valence and Rydberg levels of atoms and molecules were generally inaccessible until the advent of attosecond laser technology, which offers broad bandwidth excitation in the extreme ultraviolet (XUV) energy region and the high time resolution necessary to resolve the subsequent dynamics of widely spaced levels in such a wavepacket.

One way of studying the dynamics of these systems is attosecond transient absorption.[4] In this technique, the attosecond (as) XUV pulse creates an oscillating dipole moment between the ground and excited states of the target within its bandwidth, resulting in a time-dependent polarization. This polarization is modified by the action of a time-delayed few-femtosecond (fs) near-infrared (NIR) pulse, which can coherently couple the excited states to neighboring bound states or directly ionize states to the continuum. The interference of the original XUV pulse with this modified polarization dipole results in changes in the XUV spectrum. Superpositions of bound or autoionizing Rydberg states of atoms have been studied using this technique,[4−17] and its application to molecular species is just beginning.[18−20] In this paper, we apply attosecond transient absorption to the study of vibrational levels of multiple bound and autoionizing states of Rydberg and valence character in nitrogen between 12 and 16.7 eV.

Molecular Rydberg states with high principal quantum number n have been the target of extensive studies because the level spacing of these systems decreases with n.[21] The accessible Rydberg states in these studies are typically limited to states with n greater than 10 and are characterized by the behavior of the Rydberg electron being effectively independent of the molecular core.[21,22] Whether a general Rydberg molecule shows the same dynamics as its united core atom is an important question given that the molecular core has the ability to rotate, vibrate, and even dissociate. Some of the unique processes that are available to these molecular systems are dissociation without involvement of the Rydberg electron, vibrational autoionization, where the Rydberg electron gains

Special Issue: Ronnie Kosloff Festschrift

Received: November 26, 2015
Revised: February 9, 2016
Published: February 10, 2016

DOI: 10.1021/acs.jpca.5b11570
J. Phys. Chem. A 2016, 120, 3165−3174

the needed energy to ionize through interaction with a vibrationally excited ion core, and predissociation, where the molecule crosses to a repulsive valence potential curve.[22] The interactions of the nuclear and electronic degrees of freedom in such a system are still poorly characterized, especially for low-n Rydberg states.

Molecular nitrogen was selected as a target system to study such dynamics. The complexity of the electronic structure of N_2 in the energy range studied here, with two valence excited neutral electronic states and Rydberg states based on the ground and first two excited ion states,[23] makes it an excellent molecular target for attosecond transient absorption. A schematic showing some of the relevant potential energy curves for this investigation is presented in Figure 1.

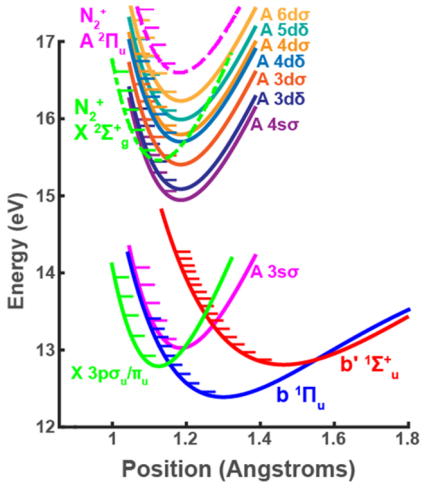

Figure 1. Nitrogen potential energy curves in the energy region of interest. The valence $b\ ^1\Pi_u$ and $b'\ ^1\Sigma^+_u$ states, the lowest Rydberg state built on the $X\ ^2\Sigma^+_g$ N_2^+ core, and Rydberg states built on the $A\ ^2\Pi_u$ N_2^+ core are indicated. The ionic $X\ ^2\Sigma^+_g$ N_2^+ (green dashed) and $A\ ^2\Pi_u$ N_2^+ (pink dashed) potentials are also shown. Potentials are adapted from ref 42.

The assignment and interactions of the nitrogen states in the 12.5 to 15 eV region has been extensively considered.[23,24] This region is dominated by vibrational progressions of the valence $b\ ^1\Pi_u$ and $b'\ ^1\Sigma^+_u$ states. These progressions are spaced in energy by ~0.1 eV, reflecting their broad potential wells offset from the equilibrium geometry of the ground state, for which the vibrational frequency is considerably larger (0.24 eV).[24] Irregularities in the intensities and vibrational spacing of these levels are explained by predissociation and the presence of the first few Rydberg states built on the $X\ ^2\Sigma^+_g$ and $A\ ^2\Pi_u$ ion cores of N_2^+.[25,26]

In contrast, there is significant debate in the literature about the assignment of the higher energy transitions in nitrogen beginning near the first ionization limit to the $v = 0$ state of $X\ ^2\Sigma^+_g$ N_2^+ at 15.559 eV.[27−40] This spectral region is expected to contain transitions to high ($v > 40$) vibrational levels of the $b'\ ^1\Sigma^+_u$ state, np Rydberg series converging to the first few vibrational levels of the ground state $X\ ^2\Sigma^+_g$ ion, ns and nd Rydberg series converging to first excited $A\ ^2\Pi_u$ ionic state at 16.697 eV, and a 3s Rydberg state built on the second excited $B\ ^2\Sigma^+_u$ ionic state.[41] For the relatively low A state Rydbergs (n = 3−8), interactions with the molecular ion core lead to crystal-field splitting of the Rydberg states, and electronic auto-ionization to the X state broadens the features such that rotational analysis becomes difficult.[34] More than 40 years of study on these features by photoabsorption, photoelectron/ion, and theoretical techniques have led to numerous and conflicting assignments, the discussion of which is outside the scope of this paper. The two most recognized assignments are by Kosman and Wallace,[28] which is consistent with previous assignments below threshold but leaves the most prominent peaks in the region of interest unassigned, and Lefebvre-Brion,[31,34,35] which assigns all of the states using three different A state Rydberg series with $ns\sigma$, $nd\sigma$, and $nd\delta$ symmetries but requires a change in the below threshold assignments for continuity. In this paper, the more complete Lefebvre-Brion assignments are used, although the debate about the assignments continues.

We find that despite the molecular nature of the autoionizing Rydberg states built on the $A\ ^2\Pi_u$ ion core that lie above the first ionization potential of nitrogen, the observed dynamics in an attosecond transient absorption measurement are remarkably atomic-like in nature and can be interpreted using a framework developed for the electronic dynamics of atomic systems.[17] We also find uniquely molecular quantum beating characteristic of nuclear-electronic superpositions in the vibrational levels of both valence states.

2. EXPERIMENTAL METHODS

Attosecond transient absorption measurements were performed on an experimental apparatus that has been described previously[43] but updated recently with interferometric control. It is depicted schematically in Figure 2. The 25 fs NIR pulses

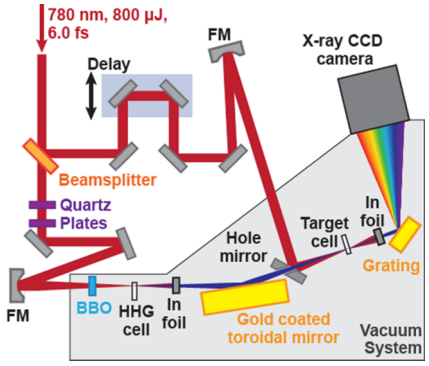

Figure 2. Attosecond transient absorption apparatus. FM = spherical focusing mirror, BBO = β-BaB_2O_4 second harmonic generation crystal, HHG = high harmonic generation. Double optical gating uses the quartz plates and BBO to manipulate the driving laser field to generate isolated attosecond pulses.

from a 2 mJ, 1 kHz titanium-sapphire laser system (HE CEP, Femtolasers) are spectrally broadened by self-phase modulation in a hollow core fiber filled with neon gas. Chirped mirrors are used to compress the output, resulting in 800 μJ, 6 fs pulses centered around 780 nm. A 70:30 beamsplitter is used to direct a majority of the beam to the generation of attosecond pulses in the XUV, while the rest is used for the few-cycle perturbative NIR pulse.

The electric field of the pulses in the XUV generation arm is reshaped using two quartz plates and a BBO crystal using a double optical gating configuration[44] that enables the production of isolated attosecond pulses from relatively long driving laser pulses. High harmonic generation is achieved by focusing this beam with a spherical mirror (f = 45 cm) into a

DOI: 10.1021/acs.jpca.5b11570
J. Phys. Chem. A 2016, 120, 3165−3174

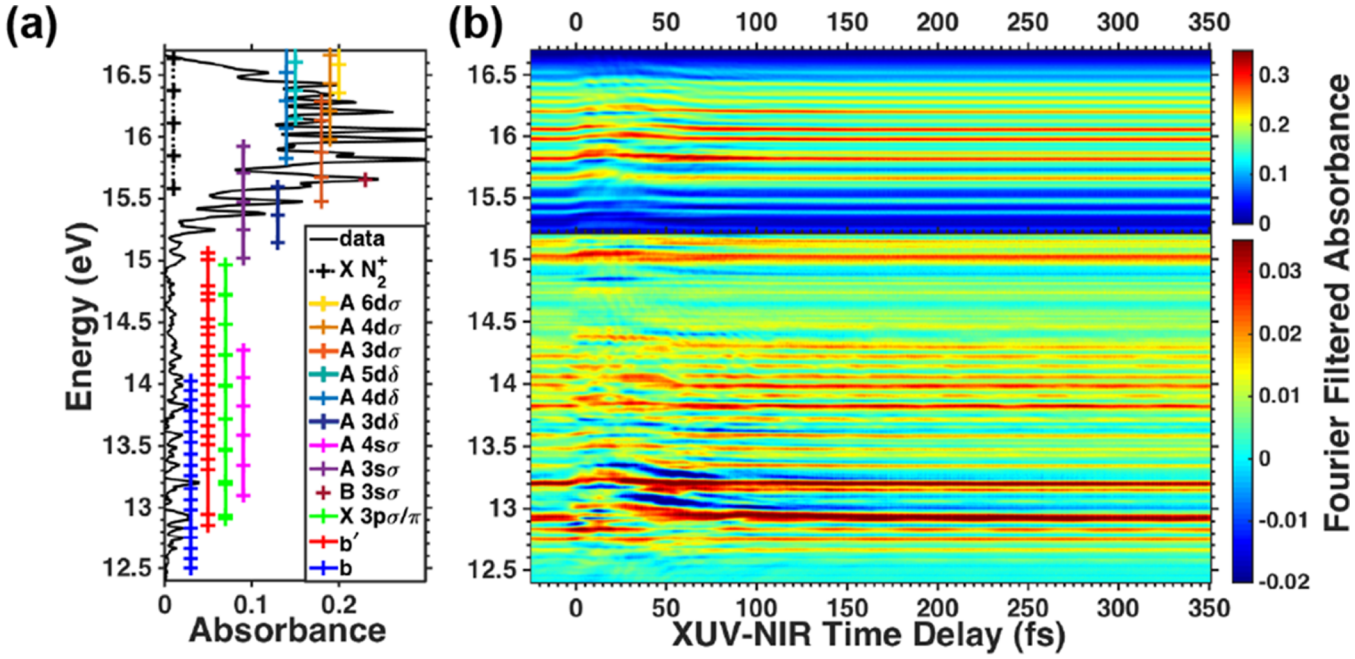

Figure 3. (a) Static absorption of nitrogen. Positions of vibrational levels of the valence $b\ ^1\Pi_u$ (blue) and $b'\ ^1\Sigma^+_u$ (red) states and of the Rydberg series built on the $X\ ^2\Sigma^+_g\ N_2^+$ (green) and $A\ ^2\Pi_u\ N_2^+$ cores are indicated.[31,34,40,47−49] (b) Nitrogen transient absorption measurement in the 12.5 to 16.7 eV photon energy range. The color scale represents absorbance that has been Fourier filtered. The NIR pulse arrives after the XUV pulse for positive time delays.

1.5 mm path length gas cell filled with xenon gas. A 200 nm indium foil blocks the residual NIR light. After passing through this filter, the XUV bandwidth is limited to 11−17 eV. The short duration and low photon energy of these attosecond pulses make exact characterization challenging. The 550 as transform limit of the measured spectrum, which has significant intensity from 14.5 to 16.5 eV and a weak tail stretching to 12 eV, is likely to underestimate the pulse duration based on previous measurements[45] because it does not account for the intrinsic chirp of the generation process or the dispersion of the generation medium.

The XUV beam is focused by a grazing incidence gold-coated toroidal mirror (f = 1 m) into the 1 mm long nitrogen target cell. The XUV photon flux is estimated to be 3×10^6 photons per pulse, corresponding to a maximum XUV intensity on the order of 10^8 W/cm^2 at the target. The NIR beam is focused using a spherical mirror (f = 1 m) and recombined with the XUV beam collinearly using an annular mirror. An adjustable delay with 100 as resolution between the two arms is produced by a piezoelectric stage in the NIR arm, allowing subcycle features to be observed. An intensity of 5×10^{12} W/cm^2 is estimated for the NIR beam at the nitrogen target based on the focusing geometry. After the interaction region, the NIR light is blocked by another 200 nm indium foil, and the XUV light is dispersed using a flat-field grating (01-0464, Hitachi) and recorded by an X-ray CCD camera (Pixis XO 400B, Princeton Instruments). Using a measurement of argon absorption lines, the spectral resolution was determined to be 19 meV at 14.3 eV.

For the nitrogen experiments, the target cell was filled with ∼200 Pascal of nitrogen gas. Each delay point is the average of three data points accumulated for 1500 laser pulses apiece. A delay step size of 300 attoseconds was used to resolve dynamics from a few to hundreds of femtoseconds with reasonable acquisition times. The grating was calibrated using the grating equation and transitions of argon and nitrogen in this energy range.[46,47] Transient absorption data are typically presented as absorbance, $A = -\log_{10}(I_{trans}/I_{ref})$, where the light transmitted by the sample is divided by a reference spectrum when there is no sample present. Because the reference is typically taken at the beginning or end of a scan, this procedure can magnify the effect of small changes in the harmonic spectrum over the course of a scan and introduce spurious noise. Fourier-filtered absorbance,[13] where the reference spectrum is constructed in situ for each time delay by a low-pass Fourier filter, eliminates this problem and improves the data statistics significantly.

3. RESULTS

The XUV pulse excites all one-photon dipole allowed states in nitrogen within its bandwidth. A static absorption spectrum with the prominent features assigned is presented in Figure 3a. The absorption of nitrogen as a function of the time delay between the attosecond XUV and few-cycle NIR pulse from 12.5 eV to the indium filter transmission edge at 16.7 eV is shown in Figure 3b. The color scale represents Fourier-filtered absorbance. The color scale has been separately assigned for regions above and below 15.2 eV, as noted in the Figure, to improve feature visibility given the large absorption that starts at this energy. Note that in the lower section the dark-blue color corresponds to emission features, which are not present in the higher energy region. The NIR pulse precedes the XUV pulse for negative time delays and follows it for positive delay times. The intensity of the NIR pulse is insufficient to affect the XUV absorption at negative delays. Thus, time zero is assigned based on the start of laser-induced changes in the nitrogen absorption features.

The delay-dependent absorption spectrum exhibits two major categories of effects. First, at delay times close to zero, many of the absorption features appear to shift to higher energies, becoming much weaker or even becoming emissive at

DOI: 10.1021/acs.jpca.5b11570
J. Phys. Chem. A 2016, 120, 3165−3174

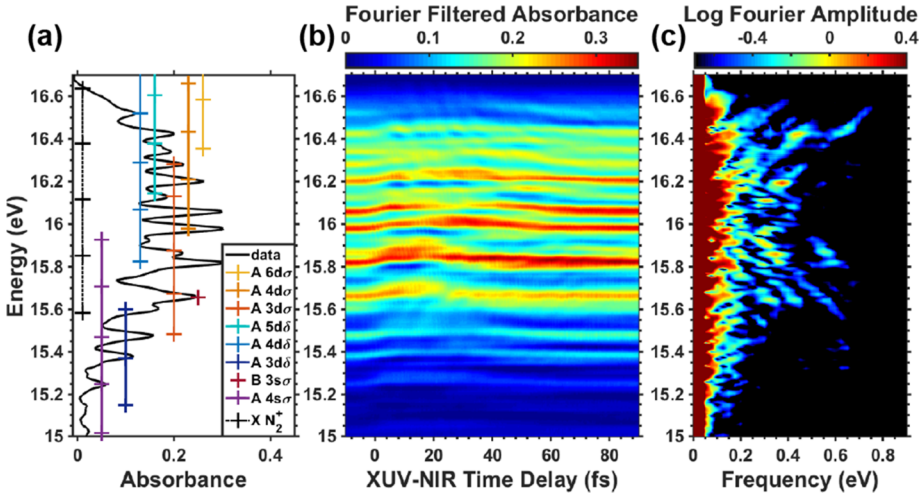

Figure 4. (a) Static absorption of nitrogen from 15 to 16.7 eV. The Lefebvre-Brion assignments are shown.[31,34] The vibrational levels of the *X* state ion are also shown for reference.[50] (b) Transient absorption spectrum in Figure 3b presented for the 15 to 16.7 eV photon energy and −10 to 90 fs time-delay range. (c) Fourier spectrum along the time axis of the absorption measurement showing the low-frequency oscillations between 0 and 0.9 eV, corresponding to beating periods greater than 4.6 fs.

the line center. For the states in the 15.3 to 16.7 eV range, the time duration of the shifting appears to vary, increasing with energy from about 20 to 80 fs. Second, in some features the absorption appears to oscillate with time. Many different oscillation periods are visible, including ∼50 fs in a feature at 12.85 eV, 5−10 fs in features at 14.5 and 16.5 eV, and 1.3 fs for features at 15.8 eV. The features above 15 eV are presented for a limited time-delay range in Figure 4b to improve visibility of the more rapid oscillations. Some of these features appear to have a positive slope (e.g., at 15.5 eV) or negative slope (e.g., at 16.5 eV) in time. The length of time over which these oscillations appear also varies by state, with some lasting for hundreds of femtoseconds while others only occur close to time zero.

To determine the period of the oscillations in the various absorption lines, we performed a Fourier transform along the time delay axis for each photon energy in the spectrum. The resulting 2D plot of state energy versus frequency (plotted in energy units of electronvolts) for the analysis of the *A* state Rydberg transient absorption region is presented separately for the frequencies from 0 to 0.8 eV in Figure 4c and from 2.5 to 3.5 eV in Figure 5a to improve the visibility of the subcycle interferences that occur in this frequency range. Similarly, the high- and low-frequency oscillations in the low-energy range, 12.4 to 13.3 eV, are presented in Figures 5b and 6c, respectively. This Fourier method is especially helpful when multiple different periods are contributing to the observed dynamics, as is the case in these energy ranges. The intermediate energy range will be considered further in a subsequent work.

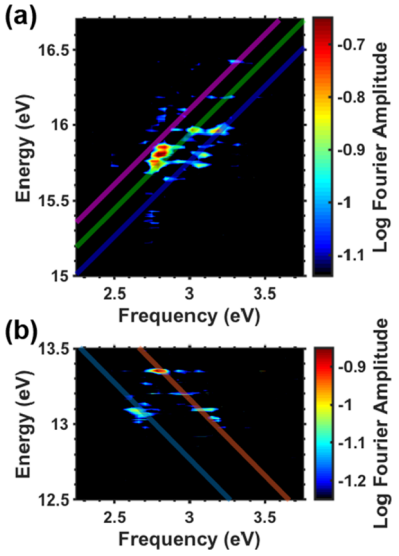

Figure 5. (a) Fourier spectrum along the time axis of the absorption measurement in the 15 to 16.7 eV photon energy range showing the high-frequency oscillations between 2.5 and 3.5 eV, corresponding to beating periods of 1.65 to 1.18 fs. (b) Fourier spectrum for 12.5 to 13.5 eV spectral range. Colored lines of slope ±1 have been added to emphasize certain contributing coupling pathways and are identified in the text.

4. ANALYSIS

Many different theoretical approaches have been developed to describe the complicated dynamics observed in attosecond transient absorption of even relatively simple atomic systems, from complete time-dependent Schrodinger approaches to simple few-level perturbative models.[7,15,51−54] Calculations for molecular species have been limited to hydrogen.[55] Thus, to aid in the understanding of the complicated and poorly characterized system of overlapping Rydberg states in nitrogen, a simplified many-level nonperturbative treatment developed for Rydberg states in argon is adapted by considering each vibrational level to be a separate state.[17]

In the dilute gas limit where the Beer−Lambert law applies, the observable in a transient absorption experiment, the absorption strength, is proportional to the imaginary part of the Fourier transform of the time dependent dipole moment. In our model, the dipole moment of a given excited state 1, $d_1(t)$, is given by

DOI: 10.1021/acs.jpca.5b11570
J. Phys. Chem. A 2016, 120, 3165−3174

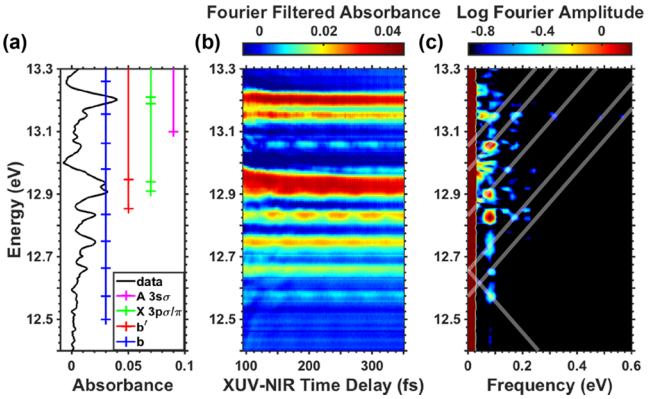

Figure 6. (a) Static absorption of nitrogen from 12.4 to 13.3 eV. Positions of vibrational levels of the valence $b\ ^1\Pi_u$ (blue) and $b'\ ^1\Sigma^+_u$ (red) states and of the Rydberg series built on the $X\ ^2\Sigma^+_g\ N_2^+$ (green) and $A\ ^2\Pi_u\ N_2^+$ (pink) cores are indicated.[31,34,40,47−49] (b) Transient absorption spectrum in Figure 3b presented for the 100−350 fs time-delay range. (c) Fourier spectrum along the time axis of the absorption measurement showing the low-frequency oscillations between 0 and 0.6 eV, corresponding to beating periods larger than 6.9 fs. Lines of slope ±1 have been added to emphasize certain contributing coupling pathways.

$$d_1(t) \propto e^{-t/t_1}\mu_{1g}^2\left[|A_1^1(t-\tau)|\sin(E_1 t + \varphi_{A_1^1}) + \sum_{n,n\neq 1}\frac{\mu_{ng}}{\mu_{1g}}|A_n^1(t-\tau)|\sin(E_1 t + \varphi_{A_n^1} + \Delta E_{n1}\tau)\right] \quad (1)$$

Here t_1 is the lifetime of the state, μ_{ng} is the dipole matrix element between state n and the ground state, τ is the relative time between the XUV and NIR pulses, E_n is the energy of state n, and $\Delta E_{n1} = E_n - E_1$. Atomic units are used throughout. The first term represents NIR-laser-induced transitions where the initial and final states are the same, in which $|A_1^1(t-\tau)|$ expresses the laser-induced depopulation of state 1 by processes like ionization and $\varphi_{A_n^1}$ is the phase corresponding to any energy shift of the state, such as would be caused by the ac Stark effect. The second term describes situations where the final and initial states do not coincide, that is, population-transfer processes. In this case, $|A_n^1(t-\tau)|$ is the magnitude of mutual population transfer and $\Delta E_{n1}\tau$ is the relative phase accumulated by state n during the different time evolution of the two coherently populated states.

To arrive at eq 1, some approximations are necessary that can limit its general applicability. Because a single active electron is assumed and no nuclear structure is included, a direct extension of this model toward molecular species is only reasonable when Rydberg states are considered. The Rydberg electrons are in relatively large orbits and thus can be assumed to have little interaction with the nuclei. At energies considerably below the ionization potential, this model is likely too simple because electron−nuclear coupling due to nonadiabatic processes is ignored. In addition, because the model assumes a time ordering where the XUV pulse resonantly populates the initial states followed by their perturbation by the NIR laser at later times, nonresonant multiphoton processes are not included. Propagation effects due to the reshaping of the XUV pulse by the medium are also neglected.

In principle, the $|A_n^1(t-\tau)|$ and $\varphi_{A_n^1}$ terms in eq 1 can include all linear and nonlinear processes that contribute to the dipole moments of each level, but it is not possible to know their exact form for such a multielectron and multiatom system under the influence of a few-cycle NIR pulse without doing a complete time-dependent calculations. However, while the complete dynamics are inaccessible, this model allows many common attosecond transient absorption phenomena such as Autler-Townes splitting, ac Stark shifts, ionization, and population transfer to be singled out and included by making rational assumptions about the formulation of these terms, in many cases by approximating them as following the time integral of the laser pulse intensity envelope.

Inspection of the expression for the dipole moment in this model reveals that population-transfer processes can cause the oscillations in absorption for specific energies. As described in the second term of eq 1, if a state with energy E_1 is coupled via a population-transfer process to a state with energy E_n, the absorption feature at E_1 will contain a term that is proportional to $\cos(\Delta E_{n,1}\ \tau)$. A Fourier transform along the delay axis will have a contribution at the frequency ω_τ when the relation $(E_n \pm \omega_\tau) = E_1$ is satisfied. Thus, in a 2D energy versus frequency Fourier spectrum, all states coupled to a particular state E_1 will appear on lines of slope ±1 from the zero-frequency energy position of state E_1.

In contrast with these persistent oscillations in the attosecond transient absorption spectrum, which can be explained in a quasi-static picture of population transfer between fixed energy levels and the resulting interferences, the line shape changes observed in the nitrogen data have their origin in the ac Stark effect, the transient reshaping of the molecular electronic structure under the influence of the few cycle NIR pulse.

Similar effects have been observed experimentally in atomic systems[6,8,14,17,54] and explained theoretically using a laser imposed phase model, where the NIR-induced coupling between a resonant excited state and other dark levels in the target results in an energy shift of the level that can be modeled as a phase shift of the time-dependent dipole moment.[52] It is included in our model as a laser-imposed phase, $\varphi_{A_1^1}$. The energy shift of the level is the ac Stark shift, and it can be broken down into resonant dipole processes that are field-cycle dependent and nonresonant quadratic Raman-type processes that follow the laser pulse envelope.[56] Resonant ac Stark shifts usually affect the XUV excited states through Rabi-type processes. In our experiment, these will likely be a small effect compared with the nonresonant processes because the NIR pulse is short, and we assume that they can be neglected. Given the large number of one-photon accessible dark states that are within the bandwidth of the NIR pulse in a typical Rydberg system, a standard approximation for the nonresonant ac Stark shift is to assume it is equivalent to the energy imparted by the ponderomotive shifting of a free electron in the NIR field.[8]

In this paper, much of the behavior observed in the transient absorption of nitrogen will be interpreted using this framework developed from atomic studies. The following sections will qualitatively discuss the population-transfer processes, and a model calculation illustrating the more complicated effects of the ac Stark term will be presented.

DOI: 10.1021/acs.jpca.5b11570
J. Phys. Chem. A 2016, 120, 3165−3174

5. DISCUSSION

5.1. Subcycle Quantum Beating. The fast, 1.3 fs period, oscillations in intensity of the various absorption lines in nitrogen visible in Figure 3b are also observed in the attosecond transient absorption spectra of atoms, most notably in Rydberg states of He,[15] Ne,[9] and Ar,[17] and in doubly excited Rydberg states of He.[13] These oscillations are caused by "which-way interference" between two energy levels in the system spaced by double the laser frequency, whereby population can be transferred between by the absorption of two NIR photons.[51] In atoms, the mechanism for these population-transfer processes is known to be highly dependent on the electronic structure of the target because the moderate intensity of the NIR pulse makes two photon transitions mediated by a resonant XUV-dipole-forbidden (dark) state more likely to be observed. A schematic illustrating this process in nitrogen is shown in Figure 7. The number and shape of the accessible

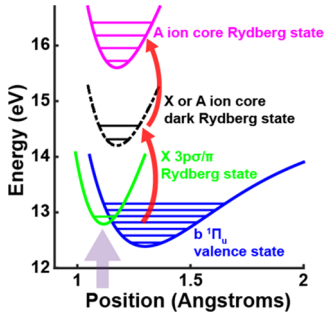

Figure 7. Schema showing the origin of the subcycle oscillations. A dark state built on the $A\ ^2\Pi_u N_2^+$ core is shown to illustrate the Franck–Condon overlap with the $b\ ^1\Pi_u$ vibrational levels. The red arrows symbolize NIR-induced population transfer. The purple arrow indicates the Franck–Condon overlap with the ground state of nitrogen.

dark states determine the magnitude of the transition dipoles that couple the bright states and will affect the strengths of the absorption oscillations through the population-transfer amplitude terms, $|A_n^1(t-\tau)|$, in eq 1. Four dark Rydberg states have been identified in the 14 eV region built on the A and X ion state cores that are good candidates to mediate the two-photon coupling pathway.[57] The two experimentally observed dark states with valence state character in nitrogen are located too low in energy to be the intermediate state for these transitions.[57−59]

In Figure 5, Fourier spectra are presented showing the relevant energy ranges giving rise to the observed subcycle dynamics. Lines have been added to guide the eyes along the dominant coupling pathways. From the positive slope of the sequence of peaks in the Fourier spectrum in Figure 5a, these states form a series that couples to states 2.5 to 3.5 eV lower in energy, causing the subcycle dynamics observed in the high-energy regime. The low photon energy regime in Figure 5b demonstrates the opposite slope when the series of points is connected; confirming that mutual coupling between these two regions is taking place. While the finite energy and frequency resolution of the experiment can lead to some uncertainties in the peak positions from the ideal lines of slope one, the observed oscillation frequencies are a substantial fraction of the XUV bandwidth and thereby limit the choice of coupling processes. The opposite tilts of the subcycle features in the low- and high-energy regions of the nitrogen transient absorption spectrum also support this interpretation.[51]

From the locations of the Fourier peaks, the most dominant coupling around 15.8 eV is from population transfer to the A state 4dδ $v = 0$ and 3dσ $v = 2$ levels from the $v = 0$ levels of the 3pσ/π Rydberg series built on the $X\ ^2\Sigma^+_g\ N_2^+$ core at 12.95 eV, illustrated by the green line in Figure 5a. These frequencies seem to be shifted slightly to lower Fourier energies than expected from the energy of the $v = 0$ 3pσ/π X state levels, almost overlapping with the $v = 0$ 3sσ A state level at 13.1 eV, which could be due to the strong energy level shifting of this feature visible in Figure 3b. Along the magenta line in Figure 5a there is also evidence of coupling between the $v = 2$ 4dσ A Rydberg state at 16.4 eV and the lowest A Rydberg state, the $v = 0$ 3sσ level at 13.1 eV. The teal and orange lines in Figure 5b show the reverse process, coupling between the $v = 0$ and 1 levels of the 3sσ A Rydberg state and the higher energy $v = 0$ 3dδ and $v = 3$ 3dσ A core Rydbergs, respectively. These sorts of population transfer between Rydberg states of differing ion cores, orbital symmetries, and sizes are observed in atomic systems.[14,17] In contrast, in Figure 5a, the oscillations at a higher frequency than the green slope of one line that is assigned to the lowest Rydberg states, the $v = 0$ 3pσ/π X state levels, must be assigned to the $v = 2$–4 vibrational levels of the $b\ ^1\Pi_u$ valence state; only the $v = 3$ level is marked with a blue line in Figure 5a for clarity. This is a first example of subcycle interferences between Rydberg and valence states.

5.2. Few-Femtosecond Quantum Beating. The few-femtosecond quantum beating visible in nitrogen has been observed analogously in atomic systems; it arises from the population transfer between two resonances close in energy via a dark state that is above or below the resonances in energy in a lambda- or vee-like coupling scheme.[14,17] This requires two NIR photons of slightly different energy, which are readily available given the 1.4 to 2.2 eV bandwidth of the few-femtosecond NIR pulse. For the A states above 15 eV in nitrogen, the four dark Rydberg states around 14 eV are good candidates to be the intermediate state in a vee-like coupling pathway.[57]

Some prominent examples of this type of beating in nitrogen are visible in the 15.85 eV level in Figure 4, which has been assigned as the 4dδ $v = 0$ state. In this state, there are 0.36 and 0.58 eV oscillations corresponding to population transfer with the 4dσ $v = 1$ and $v = 2$ levels with frequencies of 11.5 and 7 fs, respectively. In the 4dσ $v = 1$ level at 16.2 eV there is evidence of this coupling as well. While similar few-femtosecond quantum beating has been observed between electronic states in atoms,[14,17] this is the first example of such beating between vibrational levels of different electronic curves in a molecular system. A schematic of a possible vee-type coupling process for the population transfer between these states is shown in Figure 8.

There is also obvious quantum beating on a much longer time scale visible in the transient absorption of the valence states, which can be attributed to quantum beats between individual vibrational levels within these states. The dynamics of the $b\ ^1\Pi_u$ valence state between 12 and 13.2 eV are considered here, while the higher energy $b'\ ^1\Sigma_u^+$ valence state will be discussed in a separate work. The static absorption spectrum of the $b\ ^1\Pi_u$ valence state, the transient absorption spectrum for delays between 100 and 300 fs, and the Fourier analysis of this delay region are shown in Figure 6. The much faster dynamics near time zero caused by electronic coupling

DOI: 10.1021/acs.jpca.5b11570
J. Phys. Chem. A 2016, 120, 3165−3174

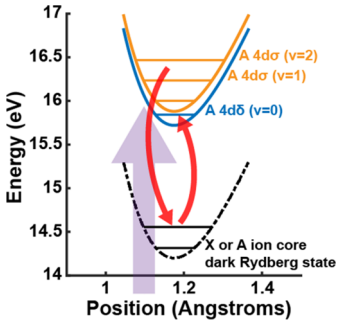

Figure 8. Schema showing the origin of the slow oscillations in the 4dδ v = 0 state at 15.85 eV. Assignments from Lefebvre-Brion are shown.[31,34] A dark state built on the A core is shown in black. The red arrows represent vee-type NIR-induced population transfer. The purple arrow indicates the Franck−Condon overlap with the ground state of nitrogen.

with these states are excluded from the Fourier analysis to focus on the slow vibrational beating. In Figure 6c there are clear peaks in the Fourier amplitude for the v = 1 to 8 levels of the b state at a frequency of 0.081 eV, corresponding to a period of 51 fs. This exactly matches the vibrational period of the b state[23] and is attributed to population transfer between vibrational states separated by $\Delta v = \pm 1$. If the spacing is uniform, we cannot distinguish between these two interference pathways (± 1); however, because of the anharmonicity of the b potential well and interactions with the lowest Rydberg states, the vibrational spacing is not constant. We can then resolve by the frequency of the observed Fourier peak which pathway is dominant. For example, the peak in the Fourier spectrum at 0.87 eV in Figure 6c reveals that the b state v = 1 level at 12.575 eV is predominantly coupled to the v = 2 level at 12.66 eV by the NIR pulse, not to the lower v = 0 level at 12.50 eV.

This coupling also extends beyond just $\Delta v = \pm 1$. Examining the v = 7 state at 13.26 eV, it is possible to see frequencies corresponding to population transfer with the v = 1, 2, 4, 5, and 6 levels. Drawing on the atomic picture, all of the vibrational quantum beats are likely caused by a similar NIR-induced vee- or lambda-type coupling through a dark state in nitrogen, as was described for the higher A states. This is illustrated in Figure 9. While the dark states previously discussed at 14 eV cannot be ruled out energetically as possibilities for mediating

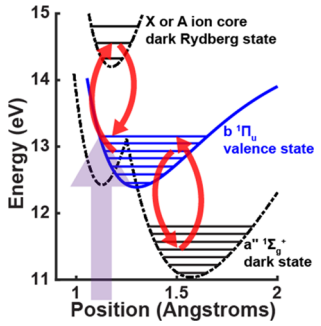

Figure 9. Schema showing the origin of the slow oscillations in the vibrational levels of the b $^1\Pi_u$ valence state. Two potential intermediate dark states are shown, a Rydberg dark state built on the A core at 14 eV and the valence a'' dark state at 11 eV. The red arrows symbolize NIR-induced population transfer. The purple arrow indicates the Franck−Condon overlap with the ground state of nitrogen.

lambda-type transitions for these b-state vibrational levels,[57] there are also theoretical predictions[42,60−62] and some experimental evidence[58,59] for a valence dark state of $^1\Sigma_g^+$ symmetry located between 11 and 12.7 eV that could be the intermediate state for a vee-type process. The vibrational quantum beating observed in this b state is a unique molecular feature, revealing nuclear-electronic coupling not present in atomic studies. Further theoretical work is currently being pursued to understand the processes that govern which population-transfer pathways contribute to the probing of these vibrational dynamics and to those of the $b'^1\Sigma_u^+$ valence state.

5.3. AC Stark Effect Model Calculation. For the purposes of simulating the effect of the ac Stark shifts on the behavior of the Rydberg states of nitrogen built on the A state core above 15 eV, we modify eq 1 to include only the laser-imposed phase. Any population-transfer processes are excluded by including only the first term in the expression. $|A_n^1(t-\tau)|$ is assumed to be unity, so ionization of these states is excluded from the model. The Rydberg electrons are presumed to be quasi-free electrons, and their phase shift is assumed to be due to the influence of an oscillating electric field treated classically as a ponderomotive shift in a monochromatic field.[8] This allows the calculation of $\varphi_{A_1^1}$ as the integral of the instantaneous energy shift, $\varphi_{A_n^1} = \int_0^t \delta E(t')\, dt'$, where $\delta E(t')$ is approximated in a monochromatic field with central frequency ω_0 and envelope $E(t)$ as $\delta E(t) = \frac{1}{2}\int_t^{-\infty} (E(t')\cos(\omega_0 t'))^2 \approx \frac{E(t)^2}{2\omega_0^2}$. Because of the complicated nature of the spectrum in this region, only the 17 apparent states in the experimental spectrum were included in the model, and their transition dipole matrix elements were estimated based on the line intensities. A lifetime of 550 fs was assumed for the states to match the value derived from the linewidths.[34] Convolution of the calculated dipole response function with a 30 meV Gaussian function mimics the experimental resolution.

The model calculated in this way for the ac Stark effect is presented with its Fourier spectrum in Figure 10. Depending on the timing of the NIR-imposed phase shift relative to the exciting XUV pulse, two different categories of dynamics can be seen. The imposed phase depends on the NIR intensity and duration, leading for specific delay times to a Lorentz to Fano or reverse transformation in the apparent spectral line shape.[8] In the calculated delay-dependent absorption spectra, these changes in the spectral line shapes manifest themselves as the apparent transient shifting of the energy levels to higher or lower energies. For longer delay times, the dipole created by the XUV pulse is allowed to freely decay for a period of time before it is modified by the laser-imposed phase. In the transient absorption spectrum, this results in a series of hyperbolic sideband features that converge on the energy level as the delay increases. The features arising from this perturbed free induction decay are universal in this type of measurement and have even been observed in optical transient absorption of semiconductors.[63] Because of the high density of Rydberg levels in nitrogen, these sideband features are only visible experimentally below the lowest excited state at 12 eV and in the apparent oscillation in the absorption of neighboring features caused when the sidebands cross them. These oscillations result in considerable contributions to the Fourier spectrum below ~0.2 eV, as is visible in the calculated spectrum shown in Figure 10b. Thus, by comparison with the ac Stark

DOI: 10.1021/acs.jpca.5b11570
J. Phys. Chem. A 2016, 120, 3165−3174

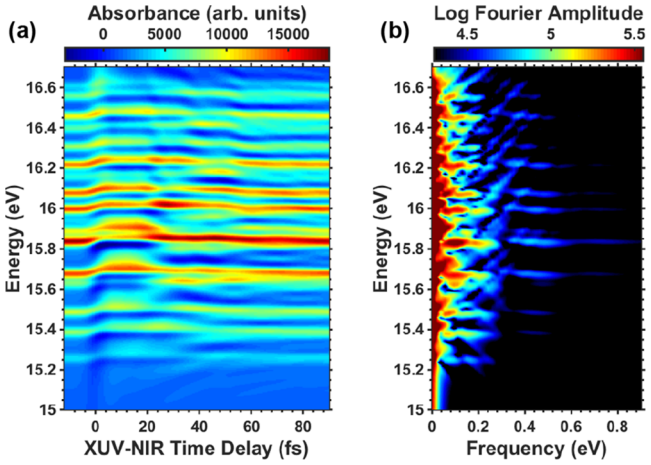

Figure 10. (a) Model absorption calculation using only the impulsive phase shift introduced by the NIR pulse in the 15 to 16.7 eV range. (b) Fourier spectrum for this model for frequencies between 0 and 0.9 eV, corresponding to beating periods larger than 4.6 fs. Comparison with Figure 4 shows that many low-frequency oscillations in the experiment can be explained by the ac Stark effect, not population transfer processes.

part of the model, the transient shifting of the energy levels to higher energies and some of the longer period quantum beating in the experimental data shown in Figure 4 are revealed to have their origins in the laser-imposed phase.

This model also reproduces the apparent increasing time duration of the disappearance of the absorption features at each resonance position as energy increases. This effect is not due to increasing lifetimes of these electronically autoionizing A state Rydbergs as their quantum numbers become larger, which has been measured using this technique in atomic systems.[5,12,16] Instead, the trend in the absorption disappearance time seems to be caused by the increasing overlap of the ac Stark shifting of the energy levels in the higher density of A Rydbergs as they approach the ionization potential. As expected in this situation, the duration of the absorption line-shifting is inversely proportional to the energy spacing between each level and the next lowest one in energy. The long lifetimes of these A core molecular Rydberg states, predicted to be 550 fs,[34] and dominance of state coupling processes over ionization of Rydberg states by the short and intense NIR pulse used here[64−66] can explain why the ac Stark shifting produces such pronounced effects in the attosecond transient absorption of these states.

6. CONCLUSIONS

Attosecond transient absorption has been used to study the ultrafast coherent dynamics of a molecular wavepacket consisting of valence and Rydberg states of nitrogen. Although most of the previous experiments using this technique have been confined to relatively simple progressions of Rydberg series in atomic species, many of the same dynamics are observed in this far more complex target.

The dynamics of the autoionizing Rydberg states built on the $A\ ^2\Pi_u\ N_2^+$ ion core above the first ionization potential of nitrogen were examined to determine whether attosecond transient absorption could resolve intrinsically coupled nuclear and electronic dynamics in these states. The small size of the Rydberg orbitals (n = 3−6), corresponding in the hydrogenic approximation to radii the same order of magnitude as the nitrogen bond length, and their low angular momentum would suggest strong interactions between the molecular ion core and the Rydberg electron; however, the observed energy level shifting of these states can be reproduced quite well by treating the Rydberg electron as a free electron in a model developed for high atomic Rydberg states. Electronic ac Stark shifting dominates the observed dynamics for these states.

Additionally, distinct quantum beats are observed due to population transfer between vibrational levels of different Rydberg states built on the $A\ ^2\Pi_u\ N_2^+$ ion core, a uniquely molecular process. Unfortunately, the lack of selectivity in the NIR-induced transitions between these states results in little insight into the difficult assignment of these states. Subcycle quantum beating is observed due to NIR-induced population transfer between energy levels in nitrogen separated by ∼3 eV. In addition to the familiar atomic-like coupling of Rydberg series built on similar ionic cores, we present the first example of such laser-induced population transfer involving molecular valence states. We also observe vibrational quantum beating in the $b\ ^1\Pi_u$ valence state between vibrational levels with $\Delta v = \pm 1$ as well as overtones corresponding to larger Δv transitions.

The observed quantum beating in nitrogen is a signature of NIR field-induced energy repartitioning between electronic and nuclear degrees of freedom, not observable in atomic transient absorption experiments. This is an inevitable consequence of field-driven quantum dynamics between bound energy levels; however, how the energy of absorbed photons is distributed into various degrees of freedom, especially in the strong field regime, is an ongoing area of research and has been shown to be a key factor in explaining the above-threshold multiphoton dissociative ionization of hydrogen.[67−69] While further theoretical work is necessary, attosecond transient absorption spectroscopy in molecular systems like nitrogen holds the promise of allowing the vibrational level-specific study and control of this energy redistribution between bound electronic states under the influence of a perturbative laser field.

In conclusion, the dynamics of a coherent molecular wavepacket prepared in nitrogen in the 12 to 16.7 eV range can mostly be interpreted using a framework built for electronic dynamics of atomic systems but show unique effects due to the addition of vibrational degrees of freedom.

AUTHOR INFORMATION

Corresponding Authors

*D.M.N.: E-mail: dneumark@berkeley.edu.
*S.R.L.: E-mail: srl@berkeley.edu.

Notes

The authors declare no competing financial interest.

ACKNOWLEDGMENTS

This work was supported by the Director, Office of Science, Office of Basic Energy Sciences and by the Division of Chemical Sciences, Geosciences, and Biosciences of the U.S. Department of Energy at LBNL under contract no. DE-AC02-05CH11231.

REFERENCES

(1) Kosloff, R.; Rice, S. A.; Gaspard, P.; Tersigni, S.; Tannor, D. J. Wavepacket Dancing: Achieving Chemical Selectivity by Shaping Light Pulses. *Chem. Phys.* **1989**, *139* (1), 201−220.
(2) Brumer, P.; Shapiro, M. Laser Control of Molecular Processes. *Annu. Rev. Phys. Chem.* **1992**, *43* (1), 257−282.

DOI: 10.1021/acs.jpca.5b11570
J. Phys. Chem. A 2016, 120, 3165−3174

(3) Rosca-Pruna, F.; Vrakking, M. Experimental Observation of Revival Structures in Picosecond Laser-Induced Alignment of I_2. *Phys. Rev. Lett.* **2001**, *87* (15), 153902.
(4) Beck, A. R.; Neumark, D. M.; Leone, S. R. Probing Ultrafast Dynamics with Attosecond Transient Absorption. *Chem. Phys. Lett.* **2015**, *624*, 119−130.
(5) Wang, H.; Chini, M.; Chen, S.; Zhang, C. H.; He, F.; Cheng, Y.; Wu, Y.; Thumm, U.; Chang, Z. Attosecond Time-Resolved Autoionization of Argon. *Phys. Rev. Lett.* **2010**, *105* (14), 143002.
(6) Chini, M.; Zhao, B.; Wang, H.; Cheng, Y.; Hu, S. X.; Chang, Z. Subcycle Ac Stark Shift of Helium Excited States Probed with Isolated Attosecond Pulses. *Phys. Rev. Lett.* **2012**, *109* (7), 073601.
(7) Chen, S.; Bell, M. J.; Beck, A. R.; Mashiko, H.; Wu, M.; Pfeiffer, A. N.; Gaarde, M. B.; Neumark, D. M.; Leone, S. R.; Schafer, K. J. Light-Induced States in Attosecond Transient Absorption Spectra of Laser-Dressed Helium. *Phys. Rev. A: At., Mol., Opt. Phys.* **2012**, *86* (6), 063408.
(8) Ott, C.; Kaldun, A.; Raith, P.; Meyer, K.; Laux, M.; Evers, J.; Keitel, C. H.; Greene, C. H.; Pfeifer, T. Lorentz Meets Fano in Spectral Line Shapes: A Universal Phase and Its Laser Control. *Science* **2013**, *340* (6133), 716−720.
(9) Wang, X.; Chini, M.; Cheng, Y.; Wu, Y.; Tong, X.-M.; Chang, Z. Subcycle Laser Control and Quantum Interferences in Attosecond Photoabsorption of Neon. *Phys. Rev. A: At., Mol., Opt. Phys.* **2013**, *87* (6), 063413.
(10) Chini, M.; Wang, X.; Cheng, Y.; Wu, Y.; Zhao, D.; Telnov, D. A.; Chu, S.-I.; Chang, Z. Sub-Cycle Oscillations in Virtual States Brought to Light. *Sci. Rep.* **2013**, *3*, 1105.
(11) Lucchini, M.; Herrmann, J.; Ludwig, A.; Locher, R.; Sabbar, M.; Gallmann, L.; Keller, U. Role of Electron Wavepacket Interference in the Optical Response of Helium Atoms. *New J. Phys.* **2013**, *15*, 1−15.
(12) Bernhardt, B.; Beck, A. R.; Li, X.; Warrick, E. R.; Bell, M. J.; Haxton, D. J.; McCurdy, C. W.; Neumark, D. M.; Leone, S. R. High-Spectral-Resolution Attosecond Absorption Spectroscopy of Autoionization in Xenon. *Phys. Rev. A: At., Mol., Opt. Phys.* **2014**, *89* (2), 023408.
(13) Ott, C.; Kaldun, A.; Argenti, L.; Raith, P.; Meyer, K.; Laux, M.; Zhang, Y.; Blättermann, A.; Hagstotz, S.; Ding, T.; et al. Reconstruction and Control of a Time-Dependent Two-Electron Wave Packet. *Nature* **2014**, *516* (18), 374−378.
(14) Beck, A. R.; Bernhardt, B.; Warrick, E. R.; Wu, M.; Chen, S.; Gaarde, M. B.; Schafer, K. J.; Neumark, D. M.; Leone, S. R. Attosecond Transient Absorption Probing of Electronic Superpositions of Bound States in Neon: Detection of Quantum Beats. *New J. Phys.* **2014**, *16* (11), 113016.
(15) Chini, M.; Wang, X.; Cheng, Y.; Chang, Z. Resonance Effects and Quantum Beats in Attosecond Transient Absorption of Helium. *J. Phys. B: At., Mol. Opt. Phys.* **2014**, *47*, 124009.
(16) Li, X.; Bernhardt, B.; Beck, A. R.; Warrick, E. R.; Pfeiffer, A. N.; Justine Bell, M.; Haxton, D. J.; William McCurdy, C.; Neumark, D. M.; Leone, S. R. Investigation of Coupling Mechanisms in Attosecond Transient Absorption of Autoionizing States: Comparison of Theory and Experiment in Xenon. *J. Phys. B: At., Mol. Opt. Phys.* **2015**, *48* (12), 125601.
(17) Cao, W.; Warrick, E. R.; Neumark, D. M.; Leone, S. R. Attosecond Transient Absorption of Argon Atoms in the Vacuum Ultraviolet Region: Line Energy Shifts versus Coherent Population Transfer. *New J. Phys.* **2016**, *18* (1), 013041.
(18) Sansone, G.; Reduzzi, M.; Dubrouil, A.; Feng, C.; Nisoli, M.; Calegari, F.; Lin, C. D.; Chu, W. C.; Poletto, L.; Frassetto, F. Attosecond Absorption Spectroscopy in Molecules. *Conf. Lasers Electro Opt. Electron. Laser Sci.* **2013**, *QF2*, QF2C.1.
(19) Cheng, Y.; Chini, M.; Wang, X.; Wu, Y.; Chang, Z. Probing Hydrogen and Deuterium Molecular Dynamics Using Attosecond Transient Absorption. In *Frontiers in Optics 2013*; OSA: Washington, DC, 2013; Vol. *1105*, p LW2H.2.
(20) Cheng, Y.; Chini, M.; Wang, X.; Wu, Y.; Chang, Z. Attosecond Transient Absorption in Molecular Hydrogen. In *CLEO: 2014*; OSA: Washington, DC, 2014; p FM2B.3.
(21) Merkt, F. Molecules in High Rydberg States. *Annu. Rev. Phys. Chem.* **1997**, *48* (1), 675−709.
(22) Freund, R. S. High-Rydberg Molecules. In *Rydberg States of Atoms and Molecules*; Stebbings, R. F., Dunning, F. B., Eds.; Cambridge University Press, 1983; pp 355−392.
(23) Gürtler, P.; Saile, V.; Koch, E. E. High Resolution Absorption Spectrum of Nitrogen in the Vacuum Ultraviolet. *Chem. Phys. Lett.* **1977**, *48* (2), 245−250.
(24) Lofthus, A.; Krupenie, P. H. The Spectrum of Molecular Nitrogen. *J. Phys. Chem. Ref. Data* **1977**, *6* (1), 113.
(25) Carroll, P. K.; Collins, C. P. High Resolution Absorption Studies of the $b^1\Pi_u \leftarrow X^1\Sigma_g^+$ System of Nitrogen. *Can. J. Phys.* **1969**, *47* (1934), 563−589.
(26) Geiger, J.; Schröder, B. Intensity Perturbations Due to Configuration Interaction Observed in the Electron Energy-Loss Spectrum of N_2. *J. Chem. Phys.* **1969**, *50* (1969), 7−11.
(27) Ogawa, M.; Tanaka, Y. Rydberg Absorption Series of N_2. *Can. J. Phys.* **1962**, *40* (11), 1593−1607.
(28) Kosman, W. M.; Wallace, S. Complete Dipole Oscillator Strength Distribution and Its Moments for N_2. *J. Chem. Phys.* **1985**, *82* (3), 1385−1399.
(29) Huber, K. P.; Jungen, C. High-Resolution Jet Absorption Study of Nitrogen near 800 A. *J. Chem. Phys.* **1990**, *92* (2), 850−861.
(30) Shaw, D. A.; Holland, D. M. P.; MacDonald, M. A.; Hopkirk, A.; Hayes, M. A.; McSweeney, S. M. A Study of the Absolute Photoabsorption Cross Section and the Photionization Quantum Efficiency of Nitrogen from the Ionization Threshold to 485 Å. *Chem. Phys.* **1992**, *166* (3), 379−391.
(31) Lefebvre-Brion, H.; Yoshino, K. Tentative Interpretation of the Rydberg Series Converging to the $A\ ^2\Pi_u$ State of N_2^+. *J. Mol. Spectrosc.* **1993**, *158* (1), 140−146.
(32) Sommavilla, M.; Hollenstein, U.; Greetham, G. M.; Merkt, F. High-Resolution Laser Absorption Spectroscopy in the Extreme Ultraviolet. *J. Phys. B: At., Mol. Opt. Phys.* **2002**, *35* (18), 3901−3921.
(33) Jungen, C.; Huber, K. P.; Jungen, M.; Stark, G. The near-Threshold Absorption Spectrum of N_2. *J. Chem. Phys.* **2003**, *118* (10), 4517.
(34) Lefebvre-Brion, H. Assignment in the near-Threshold Absorption Spectrum of N_2. *J. Chem. Phys.* **2005**, *122* (14), 144315-1−144315-6.
(35) Lefebvre-Brion, H. The "cathedral" in the near-Threshold Absorption Spectrum of N_2. *J. Electron Spectrosc. Relat. Phenom.* **2005**, *144*−*147* (14), 109−111.
(36) Sommavilla, M.; Merkt, F. On the Rotational Structure of a Prominent Band in the Vacuum-Ultraviolet Spectrum of Molecular Nitrogen. *J. Electron Spectrosc. Relat. Phenom.* **2006**, *151* (1), 31−33.
(37) Huber, K. P.; Chan, M.-C.; Stark, G.; Ito, K.; Matsui, T. N_2 Band Oscillator Strengths at near-Threshold Energies. *J. Chem. Phys.* **2009**, *131* (8), 084301.
(38) O'Keeffe, P.; Bolognesi, P.; Moise, A.; Richter, R.; Ovcharenko, Y.; Avaldi, L. Vibrationally Resolved Photoionization of N_2 Near Threshold. *J. Chem. Phys.* **2012**, *136* (10), 104307.
(39) Holland, D. M. P.; Seddon, E. A.; Daly, S.; Alcaraz, C.; Romanzin, C.; Nahon, L.; Garcia, G. A. The Effect of Autoionization on the $N_2^+X\ ^2\Sigma_g^+$ State Vibrationally Resolved Photoelectron Anisotropy Parameters and Branching Ratios. *J. Phys. B: At., Mol. Opt. Phys.* **2013**, *46* (9), 095102.
(40) Randazzo, J. B.; Croteau, P.; Kostko, O.; Ahmed, M.; Boering, K. A. Isotope Effects and Spectroscopic Assignments in the Non-Dissociative Photoionization Spectrum of N_2. *J. Chem. Phys.* **2014**, *140* (19), 194303.
(41) Yencha, A. J.; Ellis, K.; King, G. C. High-Resolution Threshold Photoelectron and Photoion Spectroscopy of Molecular Nitrogen in the 15.0−52.7eV Photon Energy Range. *J. Electron Spectrosc. Relat. Phenom.* **2014**, *195*, 160−173.
(42) Little, D. A.; Tennyson, J. An R-Matrix Study of Singlet and Triplet Continuum States of N_2. *J. Phys. B: At., Mol. Opt. Phys.* **2014**, *47* (10), 105204.

DOI: 10.1021/acs.jpca.5b11570
J. Phys. Chem. A 2016, 120, 3165−3174

(43) Bell, M.; Beck, A.; Mashiko, H.; Neumark, D. M.; Leone, S. R. Intensity Dependence of Light-Induced States in Transient Absorption of Laser-Dressed Helium Measured with Isolated Attosecond Pulses. *J. Mod. Opt.* **2013**, *60* (17), 1506−1516.
(44) Mashiko, H.; Gilbertson, S.; Li, C.; Khan, S. D.; Shakya, M. M.; Moon, E.; Chang, Z. Double Optical Gating of High-Order Harmonic Generation with Carrier-Envelope Phase Stabilized Lasers. *Phys. Rev. Lett.* **2008**, *100* (10), 103906.
(45) Mashiko, H.; Bell, M.; Beck, A.; Abel, M.; Nagel, P. M.; Steiner, C. P.; Robinson, J.; Neumark, D. M.; Leone, S. R. Tunable Frequency-Controlled Isolated Attosecond Pulses Characterized by Either 750 nm or 400 nm Wavelength Streak Fields. *Opt. Express* **2010**, *18* (25), 25887−25895.
(46) Kramida, A.; Ralchenko, Y.; Reader, J. *NIST Atomic Spectra Database* (ver. 5.1); National Insitute of Standards and Technology: Gaithersburg, MD, 2013. Available at http://physics.nist.gov/asd.
(47) Chan, W. F.; Cooper, G.; Sodhi, R. N. S.; Brion, C. E. Absolute Optical Oscillator Strengths for Discrete and Continuum Photoabsorption of Molecular Nitrogen (11−200 eV). *Chem. Phys.* **1993**, *170* (1), 81−97.
(48) Huber, K. P.; Jungen, C. High-Resolution Jet Absorption Study of Nitrogen near 800 Å. *J. Chem. Phys.* **1990**, *92* (2), 850.
(49) Moise, A.; Prince, K. C.; Richter, R. Time-Resolved Study of Excited States of N_2 near Its First Ionization Threshold. *J. Chem. Phys.* **2011**, *134* (11), 114312.
(50) Morioka, Y.; Lu, Y.; Matsui, T.; Tanaka, T.; Yoshii, H.; Hayaishi, T.; Hall, R. I. Vibrational Structure of the N_2^+ Ground State Observed by Threshold Photoelectron Spectroscopy. *J. Chem. Phys.* **1996**, *104* (23), 9357.
(51) Chen, S.; Wu, M.; Gaarde, M. B.; Schafer, K. J. Quantum Interference in Attosecond Transient Absorption of Laser-Dressed Helium Atoms. *Phys. Rev. A: At., Mol., Opt. Phys.* **2013**, *87* (3), 033408.
(52) Chen, S.; Wu, M.; Gaarde, M. B.; Schafer, K. J. Laser-Imposed Phase in Resonant Absorption of an Isolated Attosecond Pulse. *Phys. Rev. A: At., Mol., Opt. Phys.* **2013**, *88* (3), 033409.
(53) Wu, M.; Chen, S.; Gaarde, M. B.; Schafer, K. J. Time-Domain Perspective on Autler-Townes Splitting in Attosecond Transient Absorption of Laser-Dressed Helium Atoms. *Phys. Rev. A: At., Mol., Opt. Phys.* **2013**, *88* (4), 043416.
(54) Kaldun, A.; Ott, C.; Blättermann, A.; Laux, M.; Meyer, K.; Ding, T.; Fischer, A.; Pfeifer, T. Extracting Phase and Amplitude Modifications of Laser-Coupled Fano Resonances. *Phys. Rev. Lett.* **2014**, *112* (10), 103001.
(55) Bækhøj, J. E.; Yue, L.; Madsen, L. B. Nuclear-Motion Effects in Attosecond Transient-Absorption Spectroscopy of Molecules. *Phys. Rev. A: At., Mol., Opt. Phys.* **2015**, *91* (4), 1−14.
(56) Sussman, B. J.; Underwood, J. G.; Lausten, R.; Ivanov, M. Y.; Stolow, A. Quantum Control via the Dynamic Stark Effect: Application to Switched Rotational Wave Packets and Molecular Axis Alignment. *Phys. Rev. A: At., Mol., Opt. Phys.* **2006**, *73* (5), 1−14.
(57) de Lange, A.; Lang, R.; van der Zande, W.; Ubachs, W. Highly Excited States of Gerade Symmetry in Molecular Nitrogen. *J. Chem. Phys.* **2002**, *116* (18), 7893.
(58) Bominaar, J.; Schoemaecker, C.; Dam, N.; Ter Meulen, J. J.; Groenenboom, G. C. (2 + 1)REMPI on Molecular Nitrogen through the $^1\Sigma_g^+$ (II)-State. *Chem. Phys. Lett.* **2007**, *435* (4−6), 242−246.
(59) Salumbides, E. J.; Khramov, A.; Ubachs, W. High-Resolution 2 + 1 REMPI Study of the a″ $^1\Sigma_g^+$ State in N_2. *J. Phys. Chem. A* **2009**, *113* (11), 2383−2386.
(60) Ermler, W. C.; Clark, J. P.; Mulliken, R. S. Ab Initio Calculations of Potential Energy Curves and Transition Moments of $^1\Sigma^+_g$ and $^1\Sigma^+_u$ States of N_2. *J. Chem. Phys.* **1987**, *86* (1), 370.
(61) Ermler, W. C.; McLean, A. D.; Mulliken, R. S. Ab Initio Study of Valence-State Potential Energy Curves of Nitrogen. *J. Phys. Chem.* **1982**, *86* (8), 1305−1314.
(62) Hochlaf, M.; Ndome, H.; Hammoutène, D.; Vervloet, M. Valence−Rydberg Electronic States of N_2: Spectroscopy and Spin−orbit Couplings. *J. Phys. B: At., Mol. Opt. Phys.* **2010**, *43* (24), 245101.
(63) Sokoloff, J.; Joffre, M.; Fluegel, B.; Hulin, D.; Lindberg, M.; Koch, S.; Migus, A.; Antonetti, A.; Peyghambarian, N. Transient Oscillations in the Vicinity of Excitons and in the Band of Semiconductors. *Phys. Rev. B: Condens. Matter Mater. Phys.* **1988**, *38* (11), 7615−7621.
(64) Eichmann, U.; Saenz, A.; Eilzer, S.; Nubbemeyer, T.; Sandner, W. Observing Rydberg Atoms to Survive Intense Laser Fields. *Phys. Rev. Lett.* **2013**, *110* (20), 203002.
(65) Hoogenraad, J. H.; Vrijen, R. B.; Noordam, L. D. Ionization Suppression of Rydberg Atoms by Short Laser Pulses. *Phys. Rev. A: At., Mol., Opt. Phys.* **1994**, *50* (5), 4133−4138.
(66) Noordam, L. D.; Stapelfeldt, H.; Duncan, D. I.; Gallagher, T. F. Redistribution of Rydberg States by Intense Picosecond Pulses. *Phys. Rev. Lett.* **1992**, *68* (10), 1496−1499.
(67) Wu, J.; Kunitski, M.; Pitzer, M.; Trinter, F.; Schmidt, L. P. H.; Jahnke, T.; Magrakvelidze, M.; Madsen, C. B.; Madsen, L. B.; Thumm, U.; et al. Electron-Nuclear Energy Sharing in Above-Threshold Multiphoton Dissociative Ionization of H_2. *Phys. Rev. Lett.* **2013**, *111* (2), 023002.
(68) Silva, R. E. F.; Catoire, F.; Rivière, P.; Bachau, H.; Martín, F. Correlated Electron and Nuclear Dynamics in Strong Field Photoionization of H_2^+. *Phys. Rev. Lett.* **2013**, *110* (11), 113001.
(69) Yue, L.; Madsen, L. B. Characterization of Molecular Breakup by Very Intense Femtosecond XUV Laser Pulses. *Phys. Rev. Lett.* **2015**, *115* (3), 033001.

DOI: 10.1021/acs.jpca.5b11570
J. Phys. Chem. A 2016, 120, 3165−3174